

## SYNTHESIZED, CHARACTERIZATION, AND INVESTIGATED ANTIOXIDANT PROPERTIES OF NOVEL HYDRAZON COMPLEXES OF MANGANES(II), COBALT(II), NICKEL(II), COPPER(II), AND ZINC(II)

VEYAN TAHER SULEMAN\* and ABDUL GHANY M. AL-DAHER\*\*

\*Dept. of Chemistry, College of Science, University of Dohuk, ,Kurdistan Region-Iraq

\*\*Al-Noor University College, Mosul-Iraq

(Received: July 4, 2023; Accepted for Publication: August 23, 2023)

### ABSTRACT

A series of Mn(II), Co(II), Ni(II), Cu(II), and Zn(II) complexes of hydrazones derived from dibenzoyl methane and aroylhydrazines namely benzoyl hydrazine(DBMBH), 2-furoyl hydrazine (DBMFH) and picolinoyl hydrazine(DBMPH), were synthesized and characterized by elemental and thermal analysis, molar conductance, magnetic properties, IR, <sup>1</sup>H-NMR, <sup>13</sup>C-NMR, and UV-Vis spectra measurements. Spectroscopic analysis showed that the ligands acted as tridentate ONO donors to the central metal ion. Physio-chemical investigations indicate that complexes with Mn(II), Co(II), Ni (II), Cu (II), and Zn (II) have octahedral, tetrahedral, and square-planar geometries. The measurement of the molar conductance of these compounds in DMSO and in methanol revealed that they are non-electrolytic in nature. The ligand and its metal complexes were tested with DPPH to determine whether or not they have anti-oxidant action. Based on the data that was gathered, it was clear that the ligand has stronger antioxidant properties than its metal complexes.

**KEYWORD:** Transition metals, Antioxidant activity, Hydrazones, Complexes.

### 1. INTRUCTION

The condensation reaction of acid hydrazide with ketones or aldehydes produces hydrazones, which serves as a ligands in the synthesis of transition metal complexes. Because of their structural flexibility and their ability to coordinate with metals in a variety of ways, hydrazones stand out as notable domestic ligands [1]. Hydrazones are a sort of multidentate ligand because they may coordinate with a wide range of metal ions in either protonated or deprotonated species, resulting in a wide range of stable chelates with distinctive geometrical shapes [2].

Biological, clinical, medical, analytical, and pharmacological are just a few of the sectors that have benefited from the discovery and development of novel derivatives of hydrazones [3]. Numerous studies and analyses of biological activities have been conducted on hydrazone compounds with the NH-N=CH structure because of their importance in medication development [4]

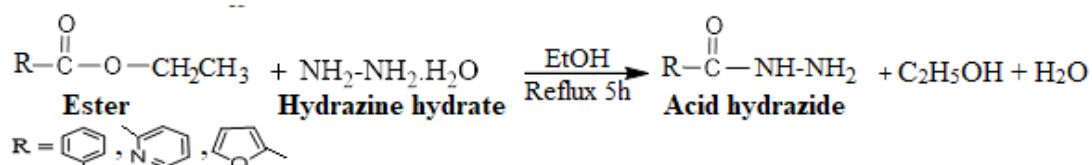
Depending on the nature of the heterocyclic ring substitutes linked to the hydrazone unit, the N- and O-donor atoms in acyl and aroyl hydrazones may coordinate with metal ions as bidentate, tridentate, tetradentate, or pentadentate ligands. The metal's coordination may be tuned by using the keto or enol versions of these ligands, which display easy keto-enol tautomerization[5].

This study is a follow-up to previous investigations into aroylhydrazones and related complexes [6], and its goals include the synthesis and characterization of novel complexes bearing the ligand term "hydrazone." Acylhydrazone contains ONO donor atoms that can be coordinated to metal ions acting as tridentates depending on the nature of the substituent attached to the hydrazone unit. These ligands exhibit an enol form, which can modulate the coordination of the metal as a di-negative ligand in enol form, as well as an assessment of their antioxidant potential.

## 2- EXPERIMENTAL

### 2.1 Equipment

The CHN analysis were carried out at the microanalytical unite elemental analyzer, CHN mode, of the university of Iran. Perkin-Elmar (AA500G) atomic absorption spectrometer photometer was used to obtain metal content. FT-IR spectra were recorded in the 4000-400  $\text{cm}^{-1}$  region fom KBr discs of the organic ligands and their complexes using Perkin-Elmer FT-IR 660 spectrophotometers. The  $^1\text{H}$  and  $^{13}\text{C}$  nuclear magnetic resonance (NMR) spectra of organic ligands were acquired on a Bruker Advance II 400. In  $\text{DMSO } d_6$  or  $\text{CDCl}_3$  ,a superconducting NMR spectrometer operating at 13000–64 MHz was used, with TMS serving as the internal standard. The UV-visible absorption spectra were measured in a quartz cell with a diameter of 1 cm and a concentration of  $10^{-3}$  M in dimethylsulfoxide in the range of 1100–200 nm using a *Unicam HEIOS* UV-VIS spectrophotometer. At a temperature of 298.5 degrees Celsius, magnetic susceptibility readings were obtained using a Johnson Matthey MSB/AUTO balance. Conductivity assessments for compounds were performed at a



### 2.2.2 Preparation of Dibenzoylmethan Hydrazone Ligands (DBMBH, DBMFH, and DBMPH)

The ligands were prepared by refluxing a mixture of acid hydrazone (0.01mole; 1.36g, 1.26g, 1.37g, of BH, FH, and PH respectively ) and dibenzoylmethan (2.24g, 0.01 mole) in 50 ml absolute ethanol for 6 hours. The volume of the solution was then reduced to 25 mL by

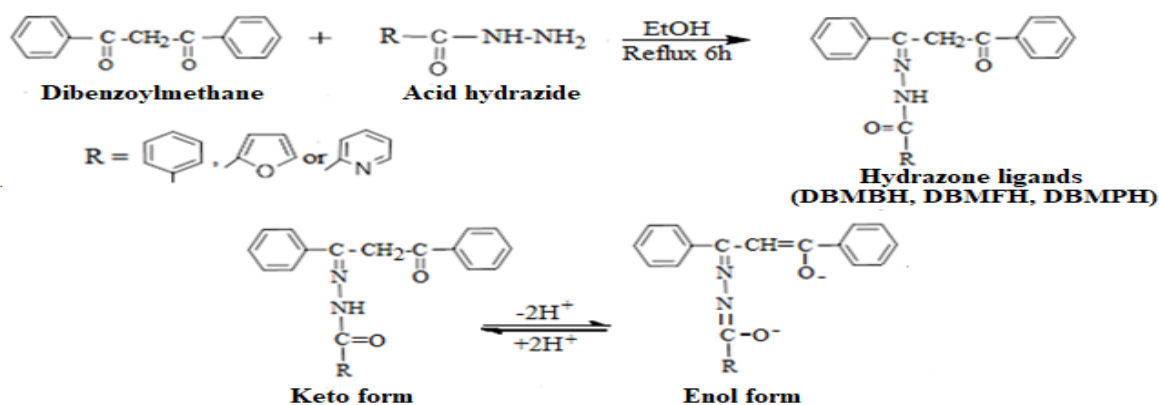
concentration of  $10^{-3}$  M in both DMSO and methanol solvents at a temperature of 25 degrees Celsius, utilizing a conductivity meter with a pH of 4.30. The thermal analyses were performed at department of chemistry, college of basic education, Mosul university using METTLER TOLEDO TGA\DSC with STARe evaluation software virgin (16.3) at 25-600°C with heat ramping rate of 5°C/min .

### 2.2 Synthesis of hydrazone ligands

#### 2.2.1 preparation of acid hydrazone (BH, FH, and PH)

The hydrazone compounds benzoyl hydrazine(BH), 2-furoyl hydrazine(FH), and picolenoyl hydrazine(PH) were made by refluxing the corresponding ester of (0.1 mole; 15.0g, 14.0g, 15.1g, Ethylbenzoate, Ethyl-2-furate and Ethylpicolenate respectively) with a slight excess of hydrazine hydrate  $\text{NH}_2\text{NH}_2 \cdot \text{H}_2\text{O}$  (6.0 g, 0.12 mole) in 50 ml of ethanol for 5 hours. The compounds were filtered and rinsed with ethanol and ether after standing overnight in freezer. The purified hydrazides were obtained by recrystallizing from hot ethanol, equation [7].

evaporating the solvent and finally cooling it in freezer. The pale yellow precipitate obtained was separated and filtered, rinsed many times with cold ethanol, and then dried in a vacuum desiccator over anhydrous  $\text{CaCl}_2$ . The ligands were recrystallized from absolute ethanol, and the reactions were confirmed using TLC on silica gel plates, Scheme (1):[8]

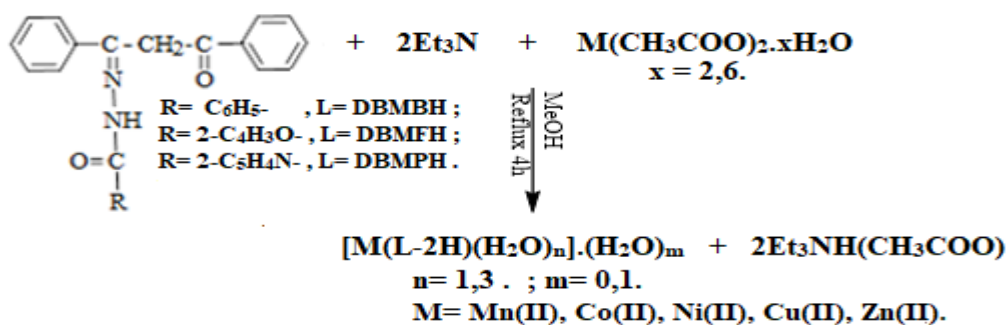


Scheme(1): synthesis of hydrazone ligands ( DBMBH, DBMFH, DBMPH)

### 2.3 Synthesis of metals complexes

To produce metal complexes, stoichiometric ratios (1:1) metal to ligands were combined. triethylamine (0.23g, 0.002 mole) was added to a heated solution of ligands (0.001mole) in 25 ml methanol, the color of solution turned yellow. A solution of metal acetate hydrate (0.001mole) in 25 ml methanol was then added.

The reaction mixtures were refluxed for 4hours, after which the volume of the solution was reduced to 20 mL and cooled in ice overnight. As shown in the equations below, the colored precipitate was separated and filtered, washed many times with cold methanol and ether, and desiccated in a vacuum desiccator over anhydrous  $\text{CaCl}_2$  (Scheme 2).[9]



Scheme (2): synthesis of metal complexes

### 2.4 Antioxidant activity of the prepared compounds:

The compounds' ability to scavenge DPPH radicals was used to determine how effective they were as antioxidants. A fresh methanol solution of DPPH (0.5mmol) was combined with the various concentrations of the investigated substances (20, 40, and 60 ppm). After 30 minutes of being held in the dark and violently shaken, the samples were analyzed.

Spectrophotometric analysis of sample absorbance at 517 nm. The following formula was used to determine the level of radical scavenging activity [10].

DPPH scavenging ability (%) =  $(\text{Abs control} - \text{Abs sample} / \text{Abs control}) * 100$

Where: Abs control = Absorbance of the DPPH radical + methanol.

Abs sample = Absorbance of the tested sample with DPPH after 30 minutes.

**Table (1):** Physical properties and analytical data of ligand and metal complexes

D=decomposed

No	Compounds	M.p. °C	Color	Yield (%)	$\Omega$ ohm <sup>1</sup> cm <sup>2</sup> mol <sup>-1</sup>		Metals % calcu./found	Elemental analysis Calcu /found		
					DMS O	Me OH		C%	H%	N%
<b>L1</b>	<b>DBMBH (C<sub>22</sub>H<sub>18</sub>N<sub>2</sub>O<sub>2</sub>)</b>	155-158	Pale yellow	87.4	----	----	-----	77.19/77.12	5.26/5.21	8.18/8.15
1	[Mn(DBMBH-2H)(H <sub>2</sub> O) <sub>3</sub> ].H <sub>2</sub> O	234-236	Black	74.2	14.9	15.6	11.75/11.61	56.54/56.32	5.14/5.02	5.99/5.64
2	[Co(DBMBH-2H)(H <sub>2</sub> O) <sub>3</sub> ]	182-185	Yellowish-brown	62.3	9.6	11.1	13.00/12.85	58.29/58.41	4.85/4.11	6.18/6.10
3	[Ni(DBMBH-2H)(H <sub>2</sub> O) <sub>3</sub> ]	250-252	Pale brown	65.1	12.2	10.2	12.96/12.45	58.31/58.01	4.85/4.10	6.18/6.02
4	[Cu(DBMBH-2H)(H <sub>2</sub> O) <sub>3</sub> ].H <sub>2</sub> O	296 d	Olive green	85.4	9.8	14.3	14.44/14.30	60.06/59.85	4.55/4.12	6.37/6.21
5	[Zn(DBMBH-2H)(H <sub>2</sub> O) <sub>3</sub> ]	136-138	Yellow	65.8	13.9	16.0	14.21/14.11	57.47/57.11	4.78/4.35	6.09/6.10
<b>L2</b>	<b>DBMFH (C<sub>20</sub>H<sub>16</sub>N<sub>2</sub>O<sub>3</sub>)</b>	118-120	Pale yellow	85.2	----	----	-----	72.28/72.17	4.81/4.65	8.43/8.40
6	[Mn(DBMFH-2H)(H <sub>2</sub> O) <sub>3</sub> ]	235-238	Dark brown	75.8	18.4	18.0	12.50/12.11	54.68/54.31	4.55/4.11	6.37/6.13
7	[Co(DBMFH-2H)(H <sub>2</sub> O) <sub>3</sub> ].H <sub>2</sub> O	162-164	Pale green	84.6	17.9	16.7	12.77/12.13	52.07/52.00	4.77/4.13	6.07/6.01
8	[Ni(DBMFH-2H)(H <sub>2</sub> O)]	269-272	Yellow-brown	87.1	19.5	13.1	14.43/14.07	59.01/58.78	3.93/3.33	6.88/6.04
9	[Cu(DBMFH-2H)(H <sub>2</sub> O) <sub>3</sub> ]	298 d	Pale green	74.3	18.5	10.1	14.18/14.00	53.63/53.02	4.46/4.32	6.25/6.06
10	[Zn(DBMFH-2H)(H <sub>2</sub> O) <sub>3</sub> ].H <sub>2</sub> O	227-229	Pale yellow	64.0	14.6	14.0	13.97/14.00	51.35/51.00	4.70/4.71	5.99/5.10
<b>L3</b>	<b>DBMPH (C<sub>21</sub>H<sub>17</sub>N<sub>3</sub>O<sub>2</sub>)</b>	160-161	Pale yellow	78.2	----	----	-----	73.46/73.24	4.95/4.76	12.24/12.24
11	[Mn(DBMPH-2H)(H <sub>2</sub> O) <sub>3</sub> ].H <sub>2</sub> O	217-210	Olive-green	69.7	12.6	18.1	11.73/11.73	53.85/53.91	4.91/4.45	8.97/8.44
12	[Co(DBMPH-2H)(H <sub>2</sub> O)] .H <sub>2</sub> O	158-159	Green-yellow	78.0	15.8	11.2	13.51/13.51	57.81/57.12	4.35/4.21	9.63/9.51
13	[Ni(DBMPH-2H)(H <sub>2</sub> O) <sub>3</sub> ]	288d	Pale brown	75.0	18.4	12.1	12.93/12.45	55.54/55.31	4.62/4.24	9.25/9.10
14	[Cu(DBMPH-2H)(H <sub>2</sub> O) <sub>3</sub> ].H <sub>2</sub> O	>300	pale olive-green	71.3	14.10	5.6	13.32/13.10	52.88/52.98	4.82/4.11	8.81/8.90
15	[Zn(DBMPH-2H)(H <sub>2</sub> O) <sub>3</sub> ]	155-158	White -yellow	74.0	12.6	18.0	14.18/14.00	54.74/54.06	4.56/4.33	9.12/9.01

### 3. REASULTS AND DISSCUSSION

The hydrazones of dibenzoylmethane (DBMBH, DBMFH and DBMPH) were synthesized in good yields by direct condensation with benzoyl hydrazine, 2-furoyl hydrazine and picolinoyl hydrazine respectively in (1:1) molar ratio in absolute ethanol (Scheme1). The reaction of these hydrazones

with metal(II) acetate in the presence of triethylamine in a molar ratio of (1:1:2) molar ratio in methanol yield 1:1 complexes in which the ligands enolized and doubly deprotonated during complexation (Scheme 2) as indicated by analytical data (Table 1). All the complexes are colored non-hygroscopic solids, stable to air and moisture at room temperature. They are generally insoluble in water and non-polar

organic solvents, soluble in ethanol, methanol, DMF and DMSO. The low molar conductance values of the complexes in methanol solutions (5.6-18.1  $\text{ohm}^{-1}\text{mol}^{-1}\text{cm}^2$ ) and in DMSO solutions (9.6-19.5  $\text{ohm}^{-1}\text{mol}^{-1}\text{cm}^2$ ) indicating the non-electrolytic nature of the complexes [11].

### 3.1 Infrared spectra studies

The IR spectra of the coordination compounds showed a range of information that was really helpful. The unique band frequencies of the ligands and the complexes containing them are listed in Table 2.

To understand the manner of bonding and the influence of the metal ion on the ligand, the IR spectra of the free ligands and their metal complexes were recorded, examined, and compared in the range 4000-400  $\text{cm}^{-1}$ . Bands at (3300, 3261, 3302), (1668, 1697, 1678) and (1635, 1646, 1656)  $\text{cm}^{-1}$  are observable in the IR spectra of the free ligands (DBMBH, DBMFH, DBMPH) are attributed to the  $\nu(\text{N-H})$ ,  $\nu(\text{C=O})$  ketone and  $\nu(\text{C=O})$  hydrazide, respectively. These were absent in the spectra of the metal complexes suggesting coordination of the enolate-form of the ligand by deprotonation of the (N-H), and ( $\text{CH}_2$ ) group during the complexation in basic medium caused by triethylamine. Carbonyl group enolization during complex formation causes this phenomenon. Evidence for the production of a new (C-O) bonds at ranges (1131-1184)  $\text{cm}^{-1}$  is consistent with the ligands being coordinated in its enolate state. Additional strong bands at (1593-1617)  $\text{cm}^{-1}$  in the infrared spectra of the free ligands are attributed to the azomethine(C=N) stretching frequency, but are shifted to lower frequency ranges (1541-1570)  $\text{cm}^{-1}$  in their complexes, showing the involvement C=N group in coordination with metal [12,13]. Coordination of nitrogen to the metal atom reduces the electron

density in the azomethine group causing a shift in the  $\nu(\text{C=N})$  band to lower frequencies. However, the (N-N) stretching vibration at (993, 928, 976,)  $\text{cm}^{-1}$  in the spectra of the free ligands respectively shifts to a higher frequency by (13-46)  $\text{cm}^{-1}$  in their complexes another indication of coordination between the metal and the nitrogen of the azomethin group [14]. The shift of (N-N) stretching vibration to higher frequencies is owing to the diminution of the lone pair electrons repulsion which comes from the two adjacent nitrogen atoms, by sharing the electrons out to the metal ion. The faint absorption bands at 617  $\text{cm}^{-1}$ , which are caused by the pyridine ring's (py) deformation vibration in free ligand(DBMPH) spectrum, were observed at almost the same or lower frequencies, indicating that the pyridine nitrogen atom was not involved in coordination in DMBPH complexes [15]. The existence of non-ligand bands in the spectra of the complexes in the ranges (457-547)  $\text{cm}^{-1}$  and (418-462)  $\text{cm}^{-1}$ , which may be tentatively assigned to (M-O) and (M-N), respectively, is another evidence that the ligand is attached to the metal ions.[16].

All complexes exhibit a broad band in their spectra centered on (3240-3392)  $\text{cm}^{-1}$  due to the symmetric and asymmetric stretching modes of the coordinated water molecules. Coordinated water molecules, furthermore gave weak bands in the (843- 940)  $\text{cm}^{-1}$  and (640- 689)  $\text{cm}^{-1}$  may represent the bending and deforming modes of coordinated water .Broad bands have also been seen in the range (3614-3736)  $\text{cm}^{-1}$  may attributed to stretching modes of uncoordinated water molecules . All the complexes had water molecules in their lattices and/or coordinated, as confirmed by thermal studies, however they all lose water when heated to 50-600°C [17, 18].

Figs (1, 2)

**Table (2):** Essential FT-IR of the ligands and their complexes

No	Chemical formula	$\nu(\text{N-H})$	$\nu(\text{C=O})$ keton	$\nu(\text{C=O})$ Hydrazide	$\nu(\text{C=N})$	$\nu(\text{C-O})$ enolic	$\nu(\text{N-N})$	$\nu(\text{M-O})$	$\nu(\text{M-N})$	(py) $\nu_{\text{end}}$ ing	$\nu(\text{H}_2\text{O})$
L1	DBMBH ( $\text{C}_{22}\text{H}_{18}\text{N}_2\text{O}_2$ )	3300	1697s	1656s	1617 sh	-----	993 w	----	-----	-----	-----
1	[Mn(DBMBH-2H)(H <sub>2</sub> O) <sub>3</sub> ].H <sub>2</sub> O	----	----	-----	1545sh	1172m	1015m	520m	443m	----	3372br, 3734br
2	[Co(DBMBH-2H)(H <sub>2</sub> O) <sub>3</sub> ]	----	----	-----	1543s	1176m	1022m	528m	447m	-----	3390br.
3	[Ni(DBMBH-2H)(H <sub>2</sub> O) <sub>3</sub> ]	----	----	-----	1550s	1180w	1022m	520w	428w	-----	3320br
4	[Cu(DBMBH-2H)(H <sub>2</sub> O)].H <sub>2</sub> O	----	----	-----	1553sh	1180m	1023m	543m	428w	-----	3322br, 3649br
5	[Zn(DBMBH-2H)(H <sub>2</sub> O) <sub>3</sub> ]	----	----	-----	1550s	1182m	1024m	524m	432w	-----	3431br.
L2	DBMFH ( $\text{C}_{20}\text{H}_{16}\text{N}_2\text{O}_3$ )	3261m	1668s	1646s	1614sh	-----	928m	-----	-----	-----	-----
6	[Mn(DBMFH-2H)(H <sub>2</sub> O) <sub>3</sub> ]	----	----	-----	1541s	1184m	941m	457m	418m	-----	3447br

7	[Co(DBMFH-2H)(H <sub>2</sub> O) <sub>3</sub> ].H <sub>2</sub> O	----	----	-----	1549s	1131m	942m	518m	418w	-----	3392br,3736br
8	[Ni(DBMFH-2H)(H <sub>2</sub> O)]	----	----	-----	1551s	1182m	941m	524m	484w	-----	3392br
9	[Cu(DBMFH-2H)(H <sub>2</sub> O) <sub>3</sub> ]	----	----	-----	1544s	1184m	945m	547m	418w	-----	3462br
10	[Zn(DBMFH-2H)(H <sub>2</sub> O) <sub>3</sub> ].H <sub>2</sub> O	----	----	-----	1549s	1132m	939m	520m	418w	-----	3391br,3650br
<b>L3</b>	<b>DBMPH (C<sub>21</sub>H<sub>17</sub>N<sub>3</sub>O<sub>2</sub>)</b>	3302m	1678m	1635s	1593s	-----	976m	-----	-----	616m	-----
11	[Mn(DBMPH-2H)(H <sub>2</sub> O) <sub>3</sub> ].H <sub>2</sub> O	----	----	-----	1552s	1172m	933m	516m	462w	613m	3355br, 3645br
12	[Co(DBMPH-2H)(H <sub>2</sub> O)].H <sub>2</sub> O	----	----	-----	1570s	1165m	1018m	520m	459w	614m	3265br, 3664br
13	[Ni(DBMPH-2H)(H <sub>2</sub> O) <sub>3</sub> ]	----	----	-----	1555s	1138m	1015m	532m	462m	615m	3246br
14	[Cu(DBMPH-2H)(H <sub>2</sub> O) <sub>3</sub> ].H <sub>2</sub> O	----	----	-----	1562sh	1180m	1022m	520w	459w	617w	3240br, 3615br
15	[Zn(DBMPH-2H)(H <sub>2</sub> O) <sub>3</sub> ]	----	----	-----	1565s	1182m	1020m	525w	443w	617m	3205br

s=strong, m= medium, w= weak, sh=shoulder, br=broad.

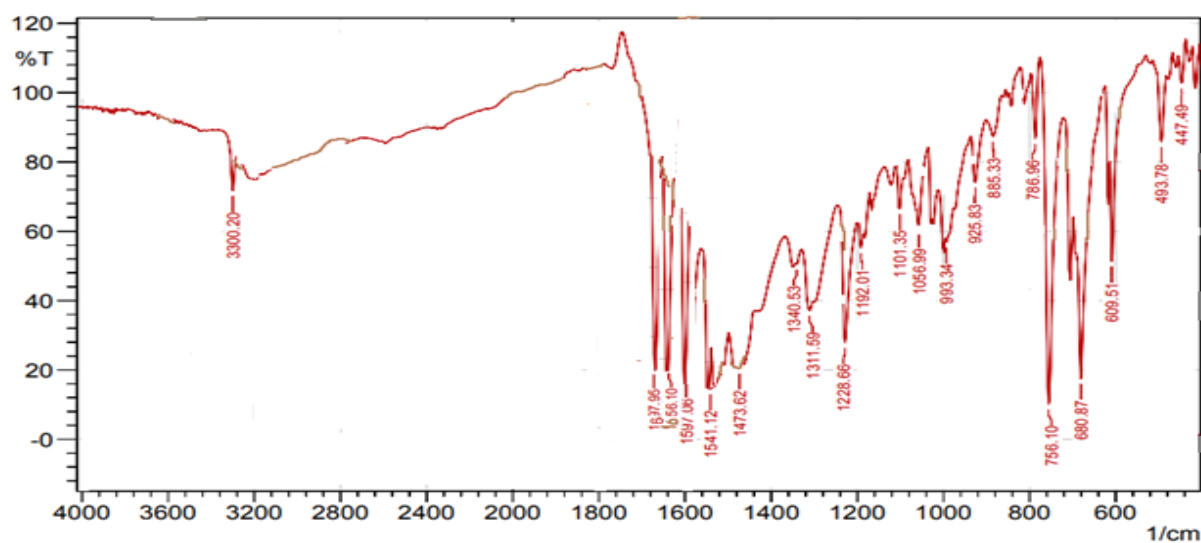


Fig. (1) IR spectrum of free ligand DBMBH

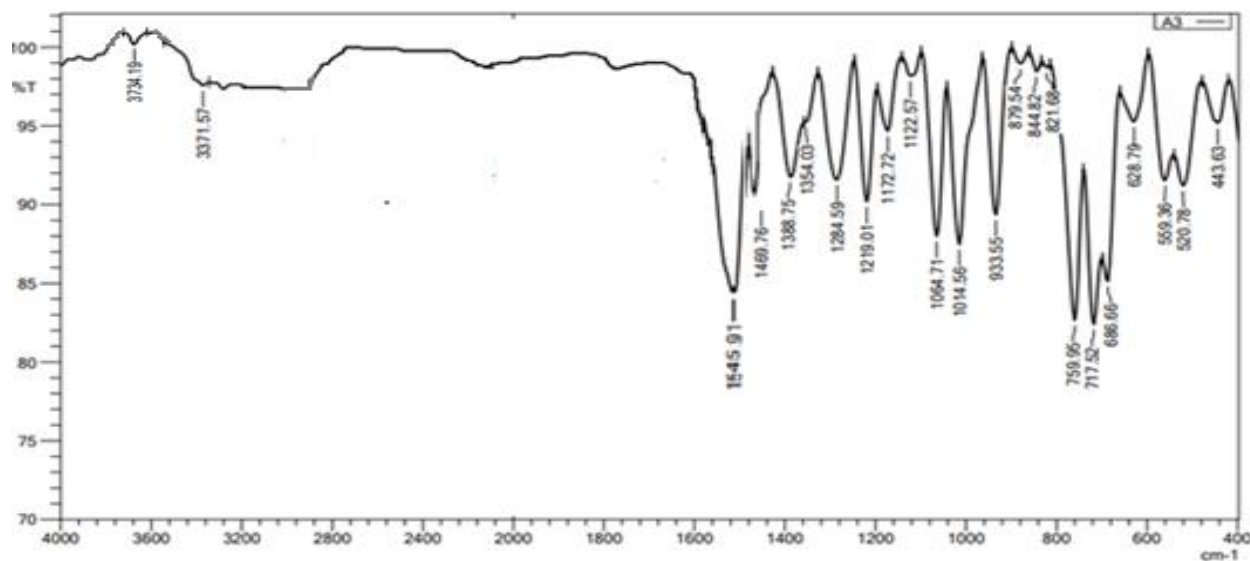


Fig.(2) IR spectrum of [Mn(DBMBH-2H)(H<sub>2</sub>O)<sub>3</sub>].H<sub>2</sub>O

### 3.2 $^1\text{H}$ and $^{13}\text{C}$ HNMR of the ligands:

In DMSO- $d_6$  and  $\text{CDCl}_3$ , the  $^1\text{H}$  and  $^{13}\text{C}$  NMR spectra of the hydrazone ligands (DBMBH, DBMFH, and DBMPH) were recorded, Fig. (3 and 4). The NH proton signal ( $1\text{H}_s, \text{NH}$ ) was detected at 10.90 -11.20 ppm, while the  $\text{CH}_2$  proton signal ( $2\text{H}_s, \text{CH}_2$ ) was seen at 4.51- 4.63 ppm. Multiple signals, corresponding to the ligands' aromatic protons in the benzene, furan, and pyridine rings, are

identified in the 6.45 -8.64-ppm range. Based on  $^{13}\text{C}$ -NMR spectroscopy,  $\text{CH}_2$  group signals are located in the range 50.4–47.3 ppm. The signals within a range of 112.0 - 148.6ppm corresponding to the ligands' aromatic carbons in the benzene, furan, and pyridine rings. Whereas  $\text{C}=\text{N}$  and  $2(\text{C}=\text{O})$  are responsible for the 145.6 - 153.7ppm and 194.8–157.8ppm signals, respectively, these findings are in line with those of previously reported compounds [19, 20].

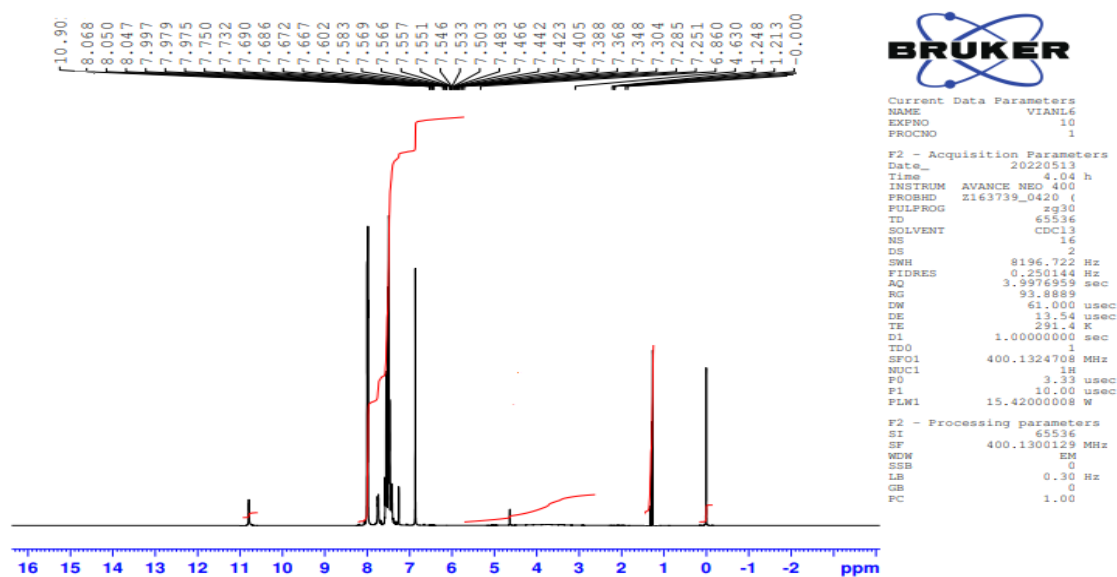


Fig.(3)  $^1\text{H}$ NMR of ligand DBMBH

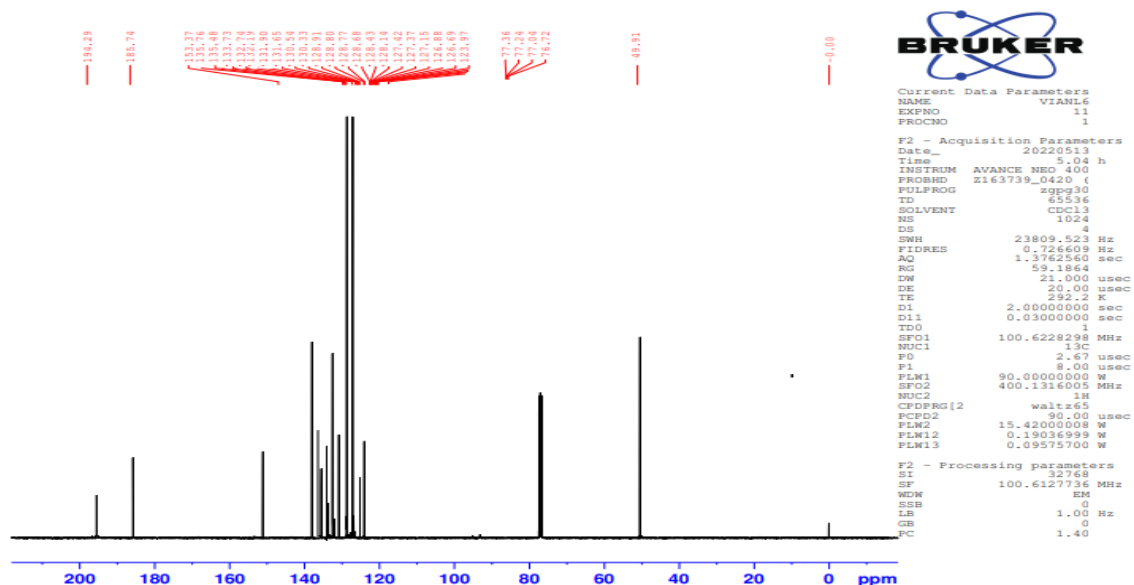


Fig. (4)  $^{13}\text{C}$  NMR of ligand DBMBH

### 3.3 Electronic spectra and magnetic studies

The electronic absorption spectra for all compounds were recorded in DMSO solution at

room temperature within the range 200-1100 nm, and the data are given in Table (3). The electronic spectral bands of free ligands

DBMBH, DBMFH, and DBMPH observed maximum absorption bands at (30030-33112)  $\text{cm}^{-1}$  and (32154–29239) corresponding to  $n \rightarrow \pi^*$  and  $\pi \rightarrow \pi^*$  respectively, as shown in Fig.(5)[21].

The spectra of the Mn(II) complexes 1, 6, and 11 appear as bands in the UV region at (27855, 26543 and 26595)  $\text{cm}^{-1}$  respectively. These bands may be assigned to  $n \rightarrow \pi^*$  and  $\pi \rightarrow \pi^*$  transition of the ligands, however, d-d transitions were not seen. These were matched with magnetic moment values of (5.7-5.9) BM, corresponding to the presence of five unpaired electrons of  $d^5$  high spin, suggesting octahedral Mn(II) complexes. [22,23].

The electronic absorption spectra of Co(II) complexes 2 and 7 visible three bands at 10344, 9794  $\text{cm}^{-1}$ , 19607, 20241  $\text{cm}^{-1}$  and 21012, 22809  $\text{cm}^{-1}$  was assigned to  ${}^4T_1g(F) \rightarrow {}^4T_2g(F)(v_1)$ ,  ${}^4T_1g(F) \rightarrow {}^4A_2g(F)(v_2)$  and  ${}^4T_1g(F) \rightarrow {}^4T_1g(P)(v_3)$ , respectively, which consists of high-spin octahedral Co(II) complexes. The magnetic moment values (5.1 and 4.6)BM for these complexes are more consistent with octahedral complexes [24,25]. Whereas the Co(II) complex (12) show band in the visible region due to d-d transitions. The band at 16949  $\text{cm}^{-1}$  is assigned to  ${}^4A_2(F) \rightarrow {}^4T_1(P)(V_3)$ , while the other transitions are not observed as they are out of the range of the used spectrophotometer. These transitions, together with a magnetic moment of  $\mu_{\text{eff}} = 4.0$  BM, reveal

that the geometry around the Co(II) ion is tetrahedral [4,26]

For the Ni(II) complexes (3) and (13), display Three bands at 9090, 1015  $\text{cm}^{-1}$ , 17094, 19010  $\text{cm}^{-1}$ , and 25641, 27777  $\text{cm}^{-1}$  correspond to  ${}^3A_2g \rightarrow {}^3T_2g(F)(v_1)$ ,  ${}^3A_2g \rightarrow {}^3T_1g(F)(v_2)$ , and  ${}^3A_2g \rightarrow {}^3T_1g(P)(v_3)$  transitions. This was consistent with (3.3 and 3.1) BM magnetic moment values confirming two unpaired electrons in an  $d^8$  octahedral Ni(II) complex [27].

The diamagnetic moment for Ni(II) complex (8) is reported for a square planar structure. Its electronic spectra show two bands at 22578 and 28760  $\text{cm}^{-1}$  assigned to  ${}^1A_1g \rightarrow {}^1A_2g(v_1)$  and  ${}^1A_1g \rightarrow {}^1B_1g(v_2)$ , respectively. these transitions reveal that the Ni(II) complexes possess a square planar geometry [28, 29].

Aboard peak observed in the visible region for Cu(II) complexes (9) and (14) within (14285, 15384)  $\text{cm}^{-1}$ . The band position with magnetic moment values (2.2 and 2.1) BM confirms the octahedral geometry of the Cu(II) ion, as shown in Fig.(6)[30]. Complex (5) display bands at 14430 and 20150  $\text{cm}^{-1}$  are corresponding to  ${}^2E_g \rightarrow {}^2T_2g$  transitions, respectively. This is confirmed with magnetic value (1.9) BM consistent with a square planer geometry around Cu(II) [31,32]. In the electronic spectra of Zn(II) complexes (6, 10, and 15) the only bands were observed due to LMCT transition[33].

**Table (3):** Magnetic moments and electronic spectral data of the complexes

No	Compound	$\mu_{\text{eff}}$ B.M	Band position $\text{cm}^{-1}$			Assignment	Geomet
1	[Mn(DBMBH-2H)(H <sub>2</sub> O) <sub>3</sub> ].H <sub>2</sub> O	5.7	27855			$n \rightarrow \pi^*$	O.h
6	[Mn(DBMFH-2H)(H <sub>2</sub> O) <sub>3</sub> ]	5.9	26543				
11	[Mn(DBMPH-2H)(H <sub>2</sub> O) <sub>3</sub> ]	5.7	26595				
2	[Co(DBMBH-2H)(H <sub>2</sub> O) <sub>3</sub> ]	5.1	10344	19607	21012	${}^4T_1g \rightarrow {}^4T_2g(F)(v_1)$ ${}^4T_1g \rightarrow {}^4A_2g(F)(v_2)$	O.h
7	[Co(DBMFH-2H)(H <sub>2</sub> O) <sub>3</sub> ].H <sub>2</sub> O	4.6	9794	20241	22809	${}^4T_1g(F) \rightarrow {}^4T_2g(P)(v_3)$	
12	[Co(DBMPH-2H)(H <sub>2</sub> O)].H <sub>2</sub> O	4.0	-----	-----	16949	${}^4A_2(F) \rightarrow {}^4T_1(P)(V_3)$	T.h
3	[Ni(DBMBH-2H)(H <sub>2</sub> O) <sub>3</sub> ]	3.3	9090	17094	25641	${}^3A_2g \rightarrow {}^3T_2g(F)(v_1)$ ${}^3A_2g \rightarrow {}^3T_1g(F)(v_2)$	O.h
13	[Ni(DBMPH-2H)(H <sub>2</sub> O) <sub>3</sub> ]	3.1	1015	19010	27777	${}^3A_2g \rightarrow {}^3T_1g(P)(v_3)$	
8	[Ni(DBMFH-2H)(H <sub>2</sub> O)]	Dia	22578	28760		${}^1A_1g \rightarrow {}^1A_2g(v_1)$ ${}^1A_1g \rightarrow {}^1B_1g(v_2)$	Sq.pl

9	[Cu(DBMFH-2H)(H <sub>2</sub> O) <sub>3</sub> ]	2.2	14285		<sup>2</sup> E <sub>g</sub> → <sup>2</sup> T <sub>2g</sub>	
14	[Cu(DBMPH-2H)(H <sub>2</sub> O) <sub>3</sub> ].H <sub>2</sub> O	2.1	15384			O.h
4	[Cu(DBMBH-2H)(H <sub>2</sub> O)]H <sub>2</sub> O	1.9	14430	20150	<sup>2</sup> B <sub>1g</sub> → <sup>2</sup> B <sub>2g</sub> <sup>2</sup> B <sub>1g</sub> → <sup>2</sup> E <sub>g</sub>	Sq.pl
5	[Zn(DBMBH-2H)(H <sub>2</sub> O) <sub>3</sub> ].H <sub>2</sub> O		26556.4			
10	[Zn(DBMFH-2H)(H <sub>2</sub> O) <sub>3</sub> ]	Dia.	243540.8		LMCT	O.h
15	[Zn(DBMPH-2H)(H <sub>2</sub> O) <sub>3</sub> ].H <sub>2</sub> O		245670.6			

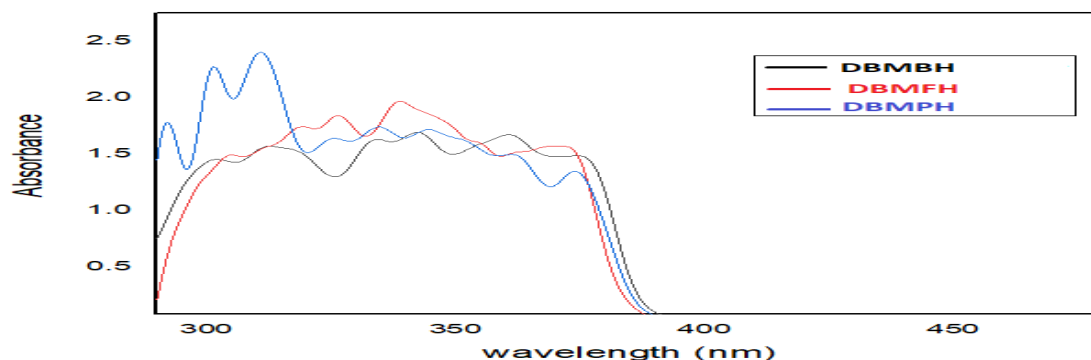
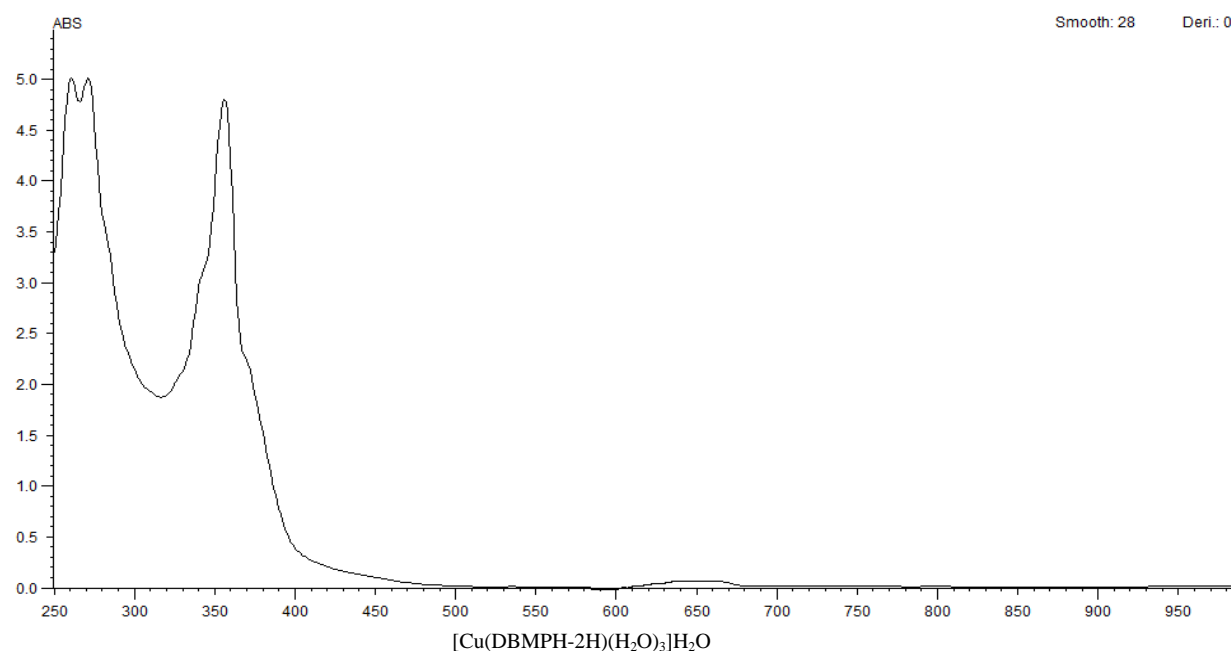


Fig. (5) Electronic spectrum of prepared ligands

Fig.(6): Electronic spectrum of [Co(DBMPH-2H)(H<sub>2</sub>O)<sub>3</sub>].H<sub>2</sub>O complex

### 3.4 Thermal analysis studies

The estimated results of thermal analysis of selected complexes was carried out at 50-600°C temperature, are shown in Table (4). The purpose of this analysis was to determine the conformation and water molecules present in the complexes as well as the type of their bonding.

Two distinct zones of losing weight can be seen in the thermograms of the undehydrated complexes (3 & 9) as in Fig (7). Three

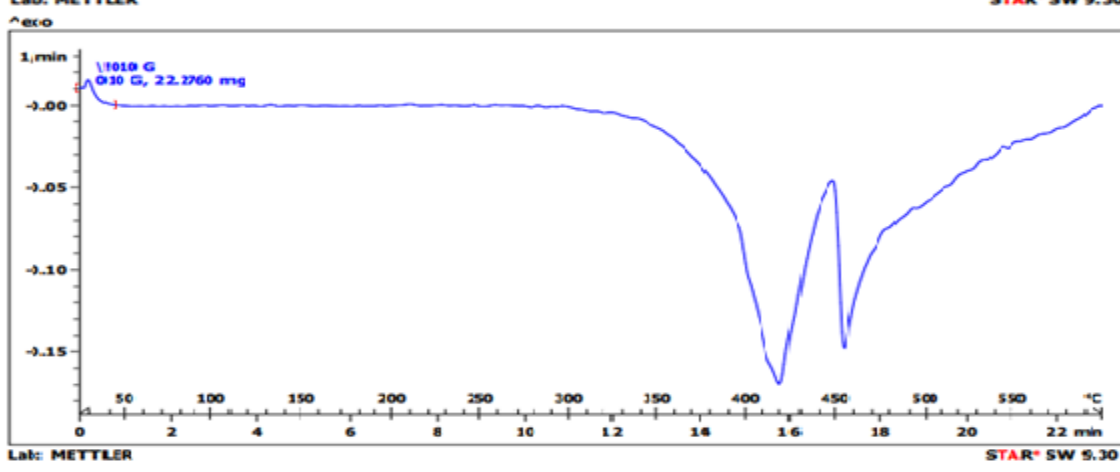
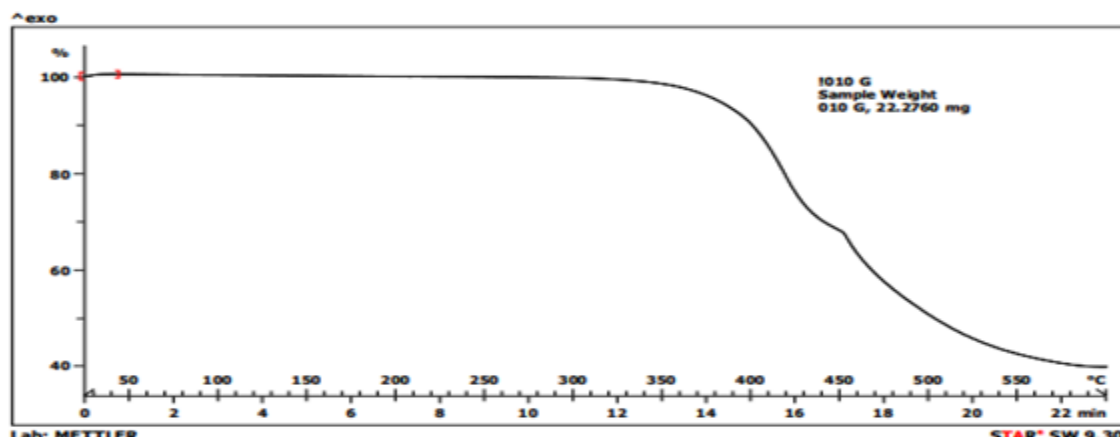
coordinated water molecules and organic fragments, C<sub>5</sub>H<sub>4</sub>ON and C<sub>10</sub>H<sub>9</sub>O<sub>2</sub>N<sub>2</sub> are released between 50-440°C, of complexes (3) and (9), respectively, as shown in the t.g.a. curves. The second stage of mass loss in these two complexes indicates that another organic component of the hydrzaone ligand is degraded in the 450-600°C region, with C<sub>10</sub>H<sub>9</sub>N and C<sub>5</sub>H<sub>5</sub> as fragments with C<sub>7</sub>H<sub>7</sub>NiO and C<sub>4</sub>CuO as residuals, respectively. It was shown through

these data that the complexes need a temperature of more than 600°C in order to obtain pure metal oxides. While there are three dissimilar areas of reduced mass in thermograms of hydrated complex (12). At low temperatures 50–115°C, complex (12) lose mass initially because 1H<sub>2</sub>O hydrate molecules in the lattice evaporate. This second stage of decomposition is attributable to

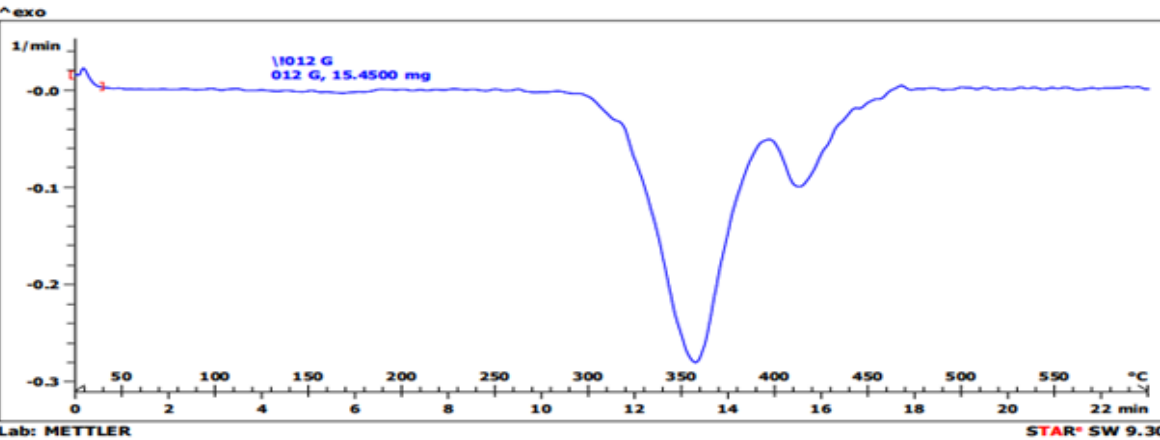
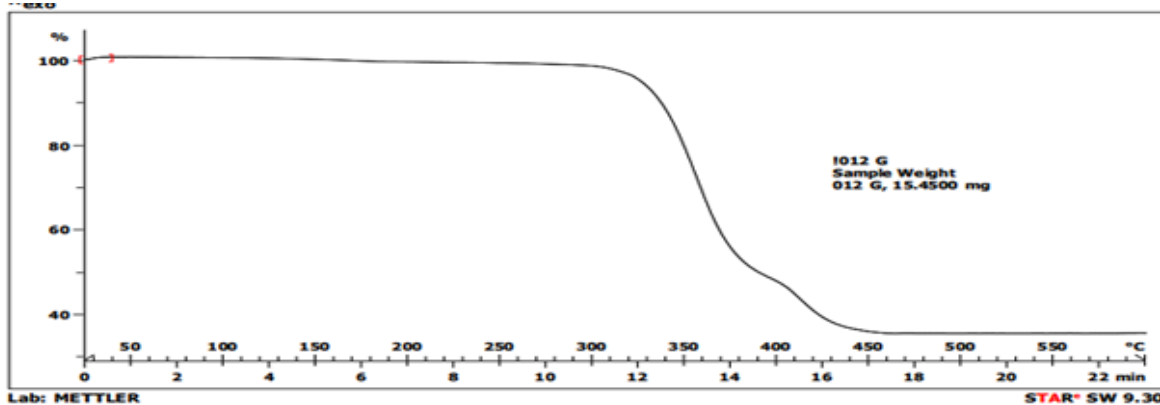
the elimination of one coordinated water (H<sub>2</sub>O) molecule and the organic fragment C<sub>10</sub>H<sub>10</sub>ON<sub>3</sub> at 120–420 °C. The third and final decomposition step for this complex (12) occurs above 450°C is metal-dependent and indicates that the organic fragment C<sub>11</sub>H<sub>5</sub> finally decomposed to CoO, as corroborated by the weight-loss results Table (4) [34,35].

**Table (4):** Thermal decomposition of some metal complexes

No	Complex	Temp. range (°C)	Estimated (calculated)	
			Massloss (%)	Assignment
3	[Ni(DBMBH-2H)(H <sub>2</sub> O) <sub>3</sub> ] C <sub>22</sub> H <sub>22</sub> O <sub>5</sub> N <sub>2</sub> Ni	50-440	31.0(32.6)	Loss of coordinated water (3H <sub>2</sub> O) and the fragment C <sub>5</sub> H <sub>4</sub> ON
		450-600	29.3(31.5)	C <sub>10</sub> H <sub>9</sub> N Residue C <sub>7</sub> H <sub>7</sub> NiO
9	[Cu(DBMFH-2H)(H <sub>2</sub> O) <sub>3</sub> ] C <sub>20</sub> H <sub>20</sub> O <sub>6</sub> N <sub>2</sub> Cu	50-440	53.0 (54.3)	Loss of coordinated water (3H <sub>2</sub> O) and fragment of C <sub>11</sub> H <sub>9</sub> O <sub>2</sub> N <sub>2</sub>
		450-600	15.0(14.5)	Loss of C <sub>5</sub> H <sub>5</sub> and residue C <sub>4</sub> CuO
12	[Co(DBMPH-2H)(H <sub>2</sub> O)]H <sub>2</sub> O C <sub>21</sub> H <sub>19</sub> O <sub>4</sub> N <sub>3</sub> Co	50–115	4.0(4.1)	Loss of hydrated (H <sub>2</sub> O)
		120-420	46.0(47.2)	Loss 1H <sub>2</sub> O coordination and fragment of C <sub>10</sub> H <sub>10</sub> ON <sub>3</sub>
		450-600	32.0(31.4)	C <sub>11</sub> H <sub>5</sub> Residue CoO



(A)



(B)

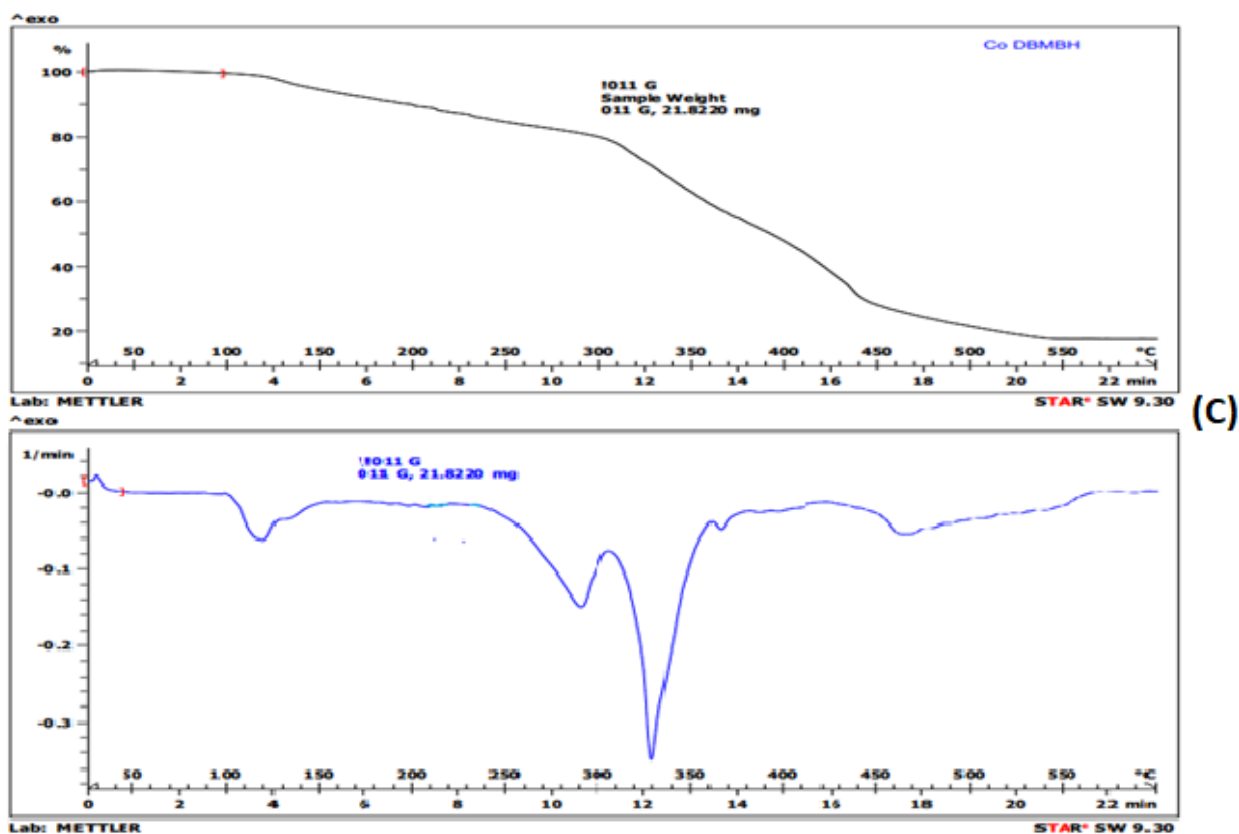


Fig.(7): TGA and DT curves of weight (%) vs. temperature (50-600°C) (a)  $[\text{Ni}(\text{DBMBH-2H})(\text{H}_2\text{O})_3]$  (b)  $[\text{Cu}(\text{DBMFH-2H})(\text{H}_2\text{O})_3]$  (c)  $[\text{Co}(\text{DBMPH-2H})(\text{H}_2\text{O})_3]\cdot\text{H}_2\text{O}$

### 3.5. Antioxidant activity of the ligand and metal complexes by DPPH

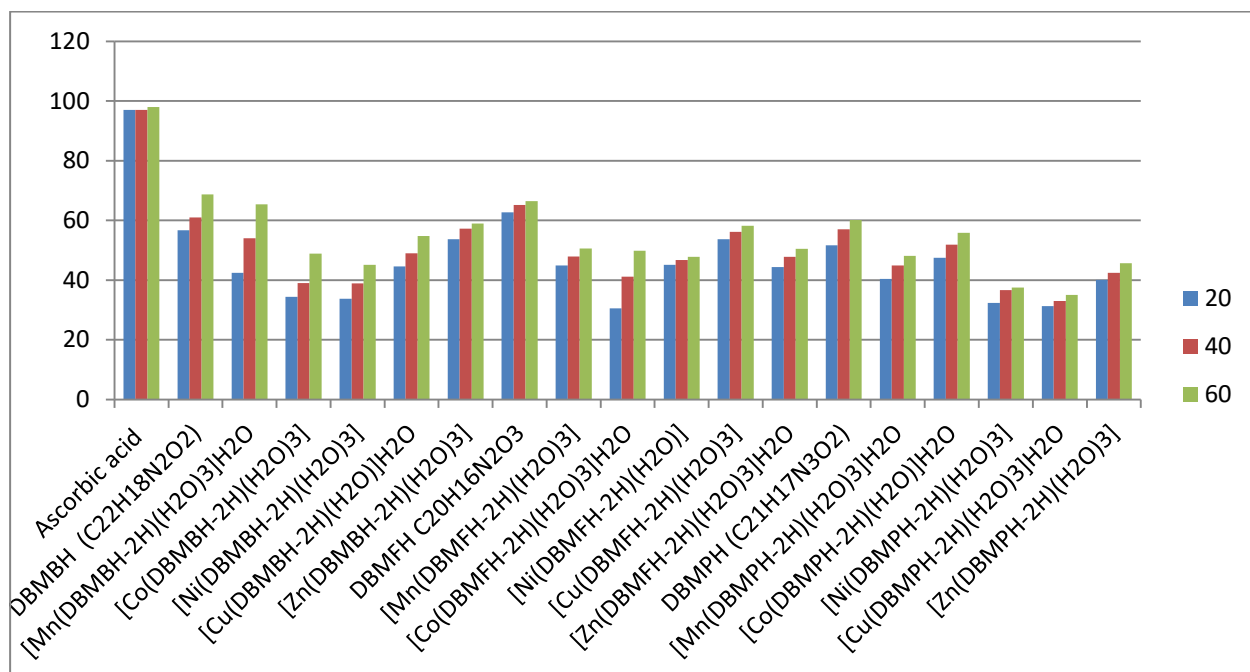
Compounds were assessed for their antioxidant activity using an evaluation technique [10]. It is generally agreed that the hydrazone compound's ability to scavenge DPPH radicals comes from its capacity to donate hydrogen.

The results effect of the free radical scavenge tested compounds at various concentrations are revealed in Fig. (8). Scavenging action of DPPH was expressed as  $\text{IC}_{50}$  the effective concentration at which 50% of the radicals were scavenged, have been calculated to assess the antioxidant activities. A lower  $\text{IC}_{50}$  indicates greater antioxidant activity. The scavenging effect of

the hydrazones and their complexes is given in Table (5). All of these compounds exhibited free radical scavenging ability at different concentrations of 20, 40, and 60 ppm as compared with the control sample (ascorbic acid). It is indicated that the ligand has much better activity of scavenging than its metal complexes. Whereas the  $[\text{Mn}(\text{DBMBH-2H})(\text{H}_2\text{O})_3]\cdot\text{H}_2\text{O}$  complex showed a strong interactive ability with DPPH among the examined complexes. While the least activity was observed from  $[\text{Cu}(\text{DBMPH-2H})(\text{H}_2\text{O})_3]\cdot\text{H}_2\text{O}$  [36]. The free radical scavenging activity of compounds depends on the structure factors and other structural features as type and geometry of metal ions [37].

**Table (5):** Antioxidant activity of the prepared compounds

standar d	Compound	Absorbance						IC <sub>50</sub> (µg/ml)
		Concentration ( µg /mL )			Antioxidant activity%			
		20	40	60	20	40	60	
	Ascorbic acid	0.035	0.032	0.019	97	97	98	44.0454
<b>L1</b>	<b>DBMBH (C<sub>22</sub>H<sub>18</sub>N<sub>2</sub>O<sub>2</sub>)</b>	0.4260	0.384	0.309	56.75	61.01	68.69	33.6898
1	[Mn(DBMBH-2H)(H <sub>2</sub> O) <sub>3</sub> ].H <sub>2</sub> O	0.567	0.453	0.340	42.43	54.01	65.42	29.1307
2	[Co(DBMBH-2H)(H <sub>2</sub> O) <sub>3</sub> ]	0.646	0.601	0.504	34.41	38.98	48.83	26.2336
3	[Ni(DBMBH-2H)(H <sub>2</sub> O) <sub>3</sub> ]	0.652	0.602	0.540	33.80	38.88	45.17	26.2336
4	[Cu(DBMBH-2H)(H <sub>2</sub> O) <sub>3</sub> ].H <sub>2</sub> O	0.546	0.502	0.445	44.56	49.03	54.82	29.853
5	[Zn(DBMBH-2H)(H <sub>2</sub> O) <sub>3</sub> ]	0.456	0.421	0.400	53.70	57.25	58.98	32.7719
<b>L2</b>	<b>DBMFH (C<sub>20</sub>H<sub>16</sub>N<sub>2</sub>O<sub>3</sub>)</b>	0.367	0.243	0.230	62.74	65.17	66.49	35.4232
6	[Mn(DBMFH-2H)(H <sub>2</sub> O) <sub>3</sub> ]	0.543	0.513	0.487	44.89	47.91	50.55	29.9633
7	[Co(DBMFH-2H)(H <sub>2</sub> O) <sub>3</sub> ].H <sub>2</sub> O	0.684	0.580	0.494	30.55	41.11	49.84	30.0566
8	[Ni(DBMFH-2H)(H <sub>2</sub> O) <sub>3</sub> ]	0.540	0.525	0.514	45.17	46.70	47.81	24.7184
9	[Cu(DBMFH-2H)(H <sub>2</sub> O) <sub>3</sub> ]	0.456	0.432	0.412	53.70	56.14	58.17	32.7719
10	[Zn(DBMFH-2H)(H <sub>2</sub> O) <sub>3</sub> ].H <sub>2</sub> O	0.546	0.514	0.488	44.36	47.81	50.45	29.7859
<b>L3</b>	<b>DBMPH (C<sub>21</sub>H<sub>17</sub>N<sub>3</sub>O<sub>2</sub>)</b>	0.476	0.423	0.386	51.67	57.05	60.08	32.1465
11	[Mn(DBMPH-2H)(H <sub>2</sub> O) <sub>3</sub> ].H <sub>2</sub> O	0.587	0.543	0.511	40.40	44.87	48.12	28.4253
12	[Co(DBMPH-2H)(H <sub>2</sub> O) <sub>3</sub> ].H <sub>2</sub> O	0.517	0.474	0.435	47.51	51.87	55.83	25.448
13	[Ni(DBMPH-2H)(H <sub>2</sub> O) <sub>3</sub> ]	0.666	0.524	0.515	32.38	36.64	37.56	30.8253
14	[Cu(DBMPH-2H)(H <sub>2</sub> O) <sub>3</sub> ].H <sub>2</sub> O	0.677	0.660	0.640	31.26	32.99	35.02	25.004
15	[Zn(DBMPH-2H)(H <sub>2</sub> O) <sub>3</sub> ]	0.435	0.413	0.400	40.10	42.43	45.68	28.3196

**Fig.(8):** Scavenging antioxidant activity of the prepared compounds

#### 4. CONCLUSION

Several Mn(II), Co(II), Ni(II), Cu(II), and Zn(II) complexes were synthesized by reacting three hydrazone ligands with the corresponding metal ions in a basic solution. The metal-to-ligand ratio was maintained at 1:1. The ligands used in the synthesis were derived from dibenzoyl methane and benzoyl hydrazine (DBMBH), 2-furoyl hydrazine (DBMFH), or picolinoyl hydrazine (DBMPH). The proposed structures of the complexes can be found in Figure 9. In this study, we concluded that the hydrazone ligands acts as a dibasic tridentate in all prepared complexes (1-15) through ONO

atoms of the azomethine nitrogen, hydrazide carbonyl and ketonic carbonyl oxygen atoms. The proposed geometry for most of the complexes is octahedral, except for complexes (4 & 8), [Cu(DBMBH-2H)(H<sub>2</sub>O)]H<sub>2</sub>O and ([Ni(DBMFH-2H)(H<sub>2</sub>O)] which are expected to have square planar structures. Additionally, complex (12) [Co(DBMPH-2H)(H<sub>2</sub>O)].H<sub>2</sub>O is proposed to have a tetrahedral geometry. The thermal stability of the compounds is closely related to their composition. Antioxidant activity against DPPH radical showed that the ligands exhibit higher radical scavenging activity than their metal complexes.

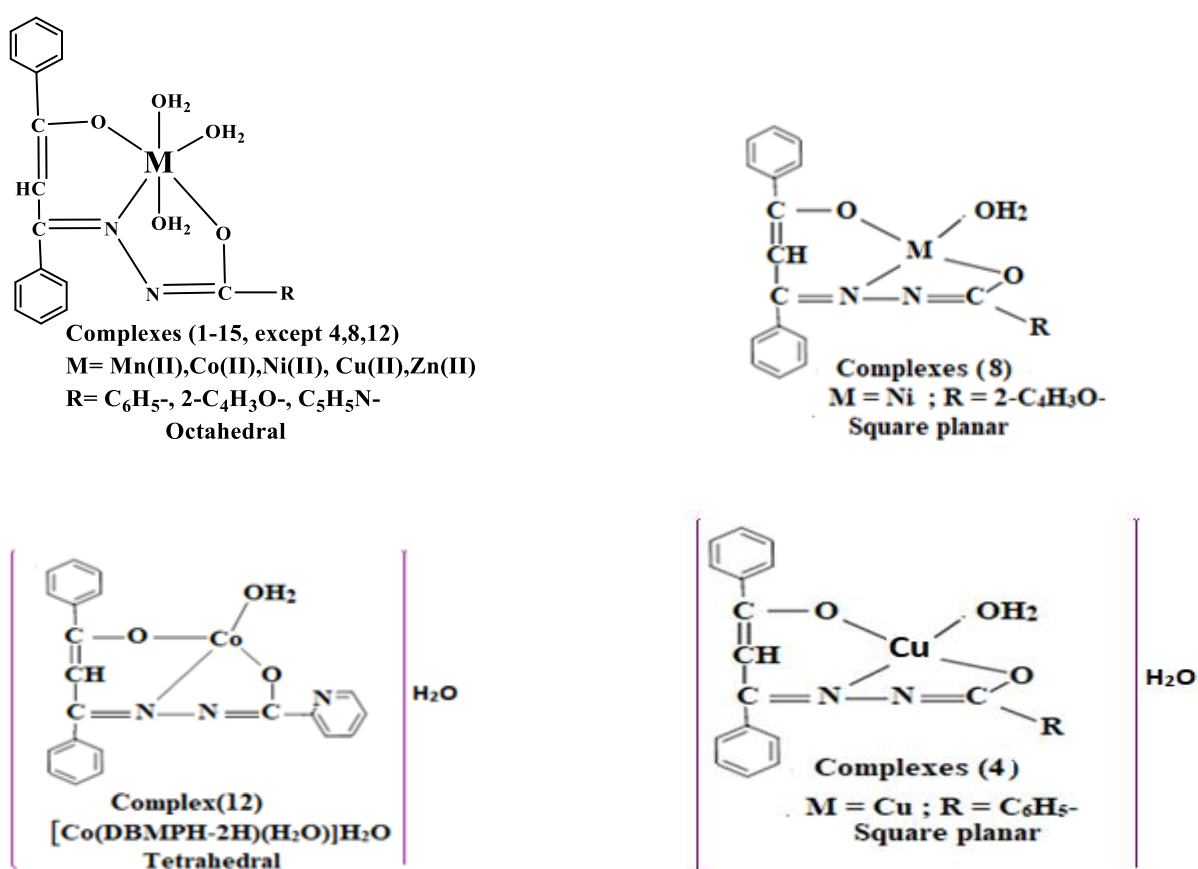


Fig. (9): Proposed structures for complexes

#### REFERENCES

- Balapoor, L., Bikas, R., & Dargahi, M. (2020). Catalytic oxidation of benzyl-alcohol with H<sub>2</sub>O<sub>2</sub> in the presence of a dioxidomolybdenum (VI) complex. *Inorganica Chimica Acta*, 510, 119734.
- Abouzayed, F. I., Emam, S. M., & Abouel-Enein, S. A. (2020). Synthesis, characterization and biological activity of nano-sized Co (II), Ni (II), Cu (II), Pd (II) and Ru (III) complexes of tetradentate hydrazone ligand. *Journal of Molecular Structure*, 1216, 128314.
- Aly, S. A., & Fathalla, S. K. (2020). Preparation, characterization of some transition metal complexes of hydrazone derivatives and their antibacterial and antioxidant activities. *Arabian Journal of Chemistry*, 13(2), 3735-3750..
- Al-Fulajj, O. A., Jeragh, B., El-Sayed, A. E. M., El-Defrawy, M. M., & El-Asmy, A. A. (2015). Chelation, spectroscopic characterization, biological activity and crystal structure of 2, 3-butanedione isonicotinylhydrazone: Determination of Zr<sup>4+</sup> after flotation

- separation. *Spectrochimica Acta Part A: Molecular and Biomolecular Spectroscopy*, 136, 1834-1841.
- Hosseini-Monfared, H., Bikas, R., Sanchiz, J., Lis, T., Siczek, M., Tucek, J., ... & Mayer, P. (2013). Syntheses, structures and magnetic properties of azido-and phenoxo-bridged complexes of manganese containing tridentate aroylhydrazone based ligands. *Polyhedron*, 61, 45-55.
- Alfares, A.A., Alnuaimy, L.A. and Al-Daher, A.G.M., (2022). Synthesis and Characterization of Mn (II), Co (II), Ni (II), Cu (II) and Zn (II) complexes with 2-Carboxy benzaldehyde Aroylhydrazones. *Egyptian Journal of Chemistry*, 65(1), pp.1-2.
- Al-Ne'aimi, M. M. (2012). Synthesis and characterization of bis-acylhydrazone derivatives as tetradentate ligands and their dinuclear metal (II) complexes. *Chem. Engineering*, 56, 83-90.
- El-Tabl, A. S., El-Saied, F. A., Plass, W., & Al-Hakimi, A. N. (2008). Synthesis, spectroscopic characterization and biological activity of the metal complexes of the Schiff base derived from phenylaminoacetohydrazide and dibenzoylmethane. *Spectrochimica Acta Part A: Molecular and Biomolecular Spectroscopy*, 71(1), 90-99.
- Al-Hakimi, A. N., El-Tabl, A. S., & Shakdofa, M. M. (2009). Coordination and biological behaviour of 2-(p-toluidino)-N'-(3-oxo-1, 3-diphenylpropylidene) acetohydrazide and its metal complexes. *Journal of Chemical Research*, 2009(12), 770-774.
- Choudhary, A., Sharma, R., Nagar, M., Mohsin, M., & Meena, H. S. (2011). Synthesis, characterization and antioxidant activity of some transition metal complexes with terpenoid derivatives. *Journal of the Chilean Chemical Society*, 56(4), 911-917.
- Jeragh, B., & El-Asmy, A. A. (2014). Coordination of Fe (III), Co (II), Ni (II), Cu (II), Zn (II), Cd (II), Hg (II), Pd (II) and Pt (II) with 2, 5-hexanedione bis (thiosemicarbazone), HBTS: crystal structure of cis-[Pd (HBTS)] Cl<sub>2</sub> and 1-(2, 5-dimethyl-1H-pyrrol-yl)-thiourea. *Spectrochimica Acta Part A: Molecular and Biomolecular Spectroscopy*, 130, 546-552.
- Bekheit, M. M., El-Shobaky, A. R., & Allah, M. T. G. (2017). Synthesis and characterization studies of new five member ring metal chelates derived from benzion phenoxyacetyl hydrazone (H2BPAH). *Arabian Journal of Chemistry*, 10, S1973-S1979.
- Sathyadevi, P., Krishnamoorthy, P., Jayanthi, E., Butorac, R. R., Cowley, A. H., & Dharmaraj, N. (2012). Studies on the effect of metal ions of hydrazone complexes on interaction with nucleic acids, bovine serum albumin and antioxidant properties. *Inorganica Chimica Acta*, 384, 83-96.
- Hosny, N. M., & Shallaby, A. H. M. (2007). Spectroscopic characterization of some metal complexes derived from 4-acetylpyridine nicotinoylhydrazone. *Transition Metal Chemistry*, 32(8), 1085-1090.
- Mitu, L., Ilis, M., Raman, N., Imran, M., & Ravichandran, S. (2012). Transition metal complexes of isonicotinoyl-hydrazone-4-diphenylaminobenzaldehyde: synthesis, characterization and antimicrobial studies. *E-Journal of Chemistry*, 9(1), 365-372.
- Patil, S. A., Unki, S. N., Kulkarni, A. D., Naik, V. H., & Badami, P. S. (2011). Synthesis, characterization, in vitro antimicrobial and DNA cleavage studies of Co (II), Ni (II) and Cu (II) complexes with ONOO donor coumarin Schiff bases. *Journal of Molecular Structure*, 985(2-3), 330-338.
- Hosny, N. M. (2011). Synthesis and Characterization of Transition Metal Complexes Derived from (E)-N-(1-(Pyridine-2-yl) ethylidene) benzohydrazide (PEBH). *Synthesis and Reactivity in Inorganic, Metal-Organic, and Nano-Metal Chemistry*, 41(7), 736-742.
- El-Tabl, A. S., El-Saied, F. A., & Al-Hakimi, A. N. (2008). Spectroscopic characterization and biological activity of metal complexes with an ONO trifunctionalized hydrazone ligand. *Journal of Coordination Chemistry*, 61(15), 2380-2401.
- Singh, Y. P., & Patel, S. K. (2021). Molecular structures, spectral, electrochemical, DFT and antioxidant activities of copper (II) complexes with NNO donor Schiff base ligand. *Journal of Molecular Structure*, 1228, 129457.
- Zhang, L., Zhang, J. P., & Zhu, D. Y. (2005). Synthesis, characterization and antibacterial activities of (N-Oxide Pyridinyl-2-Aldehyde)-3, 5-Dibenzoyloxybenzoylhydrazone and its complexes. *Synthesis and Reactivity in Inorganic, Metal-Organic and Nano-Metal Chemistry*, 35(4), 295-298.
- Sathyadevi, P., Krishnamoorthy, P., Alagesan, M., Thanigaimani, K., Muthiah, P. T., & Dharmaraj, N. (2012). Synthesis, crystal structure, electrochemistry and studies on protein binding, antioxidant and biocidal activities of Ni (II) and Co (II) hydrazone complexes. *Polyhedron*, 31(1), 294-306.
- Banerjee, S., Ray, A., Sen, S., Mitra, S., Hughes, D. L., Butcher, R. J., ... & Turner, D. R. (2008). Pseudohalide-induced structural variations in hydrazone-based metal complexes: Syntheses, electrochemical studies and structural aspects. *Inorganica Chimica Acta*, 361(9-10), 2692-2700.

- Devi, J., Batra, N., & Malhotra, R. (2012). Ligational behavior of Schiff bases towards transition metal ion and metalation effect on their antibacterial activity. *Spectrochimica Acta Part A: Molecular and Biomolecular Spectroscopy*, 97, 397-405.
- Mohapatra, R. K., Dash, M., Mishra, U. K., Mahapatra, A., & Dash, D. C. (2014). Synthesis, spectral characterization, and fungicidal activity of transition metal complexes with benzimidazolyl-2-hydrazones of glyoxal, diacetyl, and Benzil. *Synthesis and Reactivity in Inorganic, Metal-Organic, and Nano-Metal Chemistry*, 44(5), 642-648.
- Kanchanadevi, S., Fronczek, F. R., David, C. I., Nandhakumar, R., & Mahalingam, V. (2021). Investigation of DNA/BSA binding and cytotoxic properties of new Co (II), Ni (II) and Cu (II) hydrazone complexes. *Inorganica Chimica Acta*, 526, 120536.
- Mangalam, N. A., Kurup, M. P., Suresh, E., Kaya, S., & Serdaroglu, G. (2021). Diversities in the chelation of aroylhydrazones towards cobalt (II) salts: synthesis, spectral characterization, crystal structure and some theoretical studies. *Journal of Molecular Structure*, 1232, 129978..
- Singh, V. P., Singh, S., Singh, D. P., Singh, P., Tiwari, K., Mishra, M., & Butcher, R. J. (2013). Synthesis, spectral and single crystal X-ray diffraction studies on Co (II), Ni (II), Cu (II) and Zn (II) complexes with o-amino acetophenone benzoyl hydrazone. *Polyhedron*, 56, 71-81.
- Sharma, A. K., & Chandra, S. (2013). Synthesis, structural and fungicidal studies of hydrazone based coordination compounds. *Spectrochimica Acta Part A: Molecular and Biomolecular Spectroscopy*, 103, 96-100.
- Özdemir, Ü. Ö., Akkaya, N., & Özbek, N. (2013). New nickel (II), palladium (II), platinum (II) complexes with aromatic methanesulfonylhydrazone based ligands. Synthesis, spectroscopic characterization and in vitro antibacterial evaluation. *Inorganica Chimica Acta*, 400, 13-19.
- Rakha, T. H., El-Gammal, O. A., Metwally, H. M., & El-Reash, G. A. (2014). Synthesis, characterization, DFT and biological studies of (Z)-N'-(2-oxoindolin-3-ylidene) picolinohydrazide and its Co (II), Ni (II) and Cu (II) complexes. *Journal of Molecular Structure*, 1062, 96-109.
- Singh, P. K., & Kumar, D. N. (2006). Spectral studies on cobalt (II), nickel (II) and copper (II) complexes of naphthaldehyde substituted aroylhydrazones. *Spectrochimica Acta Part A: Molecular and Biomolecular Spectroscopy*, 64(4), 853-858..
- El-Motaleb, A., Ramadan, M., & Issa, R. M. (2005). Synthesis, characterization and ascorbic acid oxidase mimetic catalytic activity of copper (II) picolyl hydrazone complexes. *Transition metal chemistry*, 30, 471-480.
- Santiago, P. H., Santiago, M. B., Martins, C. H., & Gatto, C. C. (2020). Copper (II) and zinc (II) complexes with Hydrazone: Synthesis, crystal structure, Hirshfeld surface and antibacterial activity. *Inorganica Chimica Acta*, 508, 119632.
- Al-Hazmi, G. A., & El-Asmy, A. A. (2009). Synthesis, spectroscopy and thermal analysis of copper (II) hydrazone complexes. *Journal of Coordination Chemistry*, 62(2), 337-345.
- Elsayed, S. A., Butler, I. S., Claude, B. J., & Mostafa, S. I. (2015). Synthesis, characterization and anticancer activity of 3-formylchromone benzoylhydrazone metal complexes. *Transition Metal Chemistry*, 40, 179-187..
- Saleh, R. A., Mohammad, H. A., & Saber, S. N. A. (2020). New Mixed Ligand Cobalt (II), Nickel (II) and Copper (II) Complexes of 2, 2'-Bipyridine-3, 3'-Dicarboxylic acid (bpdc) with 2-Mercapto-5-Phenyl-1, 3, 4-Oxadiazole (phozSH) and Their Antioxidant activity. *Oriental Journal of Chemistry*, 36(5), 834.
- Zhang, L., & Tang, N. (2007). Synthesis and Characterization of Benzoyl Vanillin Hydrazone and its Complexes with Biological Activities. *Synthesis and Reactivity in Inorganic, Metal-Organic and Nano-Metal Chemistry*, 37(3), 185-188.